ORIGINAL RESEARCH

Food Science & Nutrition

WILEY

Metabolomics study of *Angelica sinensis* (Oliv.) Diels on the abnormal uterine bleeding rats by ultra-performance liquid chromatography–quadrupole–time-of-flight mass spectrometry analysis

Ting-Ting Chen[1,2] | Liang Zou[3] | Di Wang[4] | Wei Li[5] | Yong Yang[5] | Xiao-Min Liu[2] | Xin Cao[5] | Jia-Rong Chen[5] | Yan Zhang[5] | Jia Fu[1]

[1]Affiliated Hospital of Chengdu University, Chengdu University, Chengdu, China

[2]School of Pharmacy, Dali University, Dali, China

[3]Key Laboratory of Coarse Cereal Processing of Ministry of Agriculture and Rural Affairs, School of Food and Biological Engineering, Chengdu University, Chengdu, China

[4]School of Pharmacy, Chengdu University of Traditional Chinese Medicine, Chengdu, China

[5]School of Preclinical Medicine, Chengdu University, Chengdu, China

Correspondence
Yan Zhang and Jia Fu, School of Preclinical Medicine, Affiliated Hospital of Chengdu University, Chengdu University, Chengdu, China.
Emails: zhangyan@cdu.edu.cn (YZ); fujia@cdu.edu.cn (JF)

Funding information
Health and Family Planning Commission of Chengdu-Key disciplines of clinical pharmacy; Sichuan Medical Research Project, Grant/Award Number: S18056; Sichuan Medical Research Project, Grant/Award Number: S19030

Abstract

The objective of this study was to explore the effects and underlying intervention mechanisms of *Angelica* water extract (AWE) on abnormal uterine bleeding (AUB) based on serum metabolomics. Firstly, the concentration of main active substances in AWE was determined and the chemical components were identified by UPLC-Q-Exactive Orbitrap-MS/MS. A drug-induced abortion model was established by mifepristone and misoprostol. After administration AWE (2.16 g/kg) for 7 days, the coagulation function, serum hormone levels, H&E staining, and immunohistochemistry observation of uterus were detected. In addition, serum metabolites profiles were performed on ultra-performance liquid chromatography–quadrupole–time-of-flight mass spectrometry (UPLC-Q-TOF-MS). The contents of ferulic acid, senkyunolide A, and ligustilide in AWE were 0.7276, 0.0868, and 1.9908 mg/g, respectively. Twenty-six compounds were identified in AWE. It was found that AWE was effective in regulation of coagulation function and promoting endometrial recovery. Meanwhile, the levels of E_2, Pg, and HCG and the expression of ERα, Erβ, and PR were down-regulated in AUB model and up-regulated by the treatment of AWE. Twenty-one potential biomarkers were eventually identified by multivariate statistical analysis. Study indicated that glycerophospholipid, sphingolipid, amino acids, retinol metabolism and primary bile acid biosynthesis were the main related metabolic pathways involved for the treatment of AUB by AWE. The results showed that AWE has potential therapeutic effect on AUB by altering the metabolic aberrations.

KEYWORDS
abnormal uterine bleeding, Angelica water extract, metabolomics, UPLC-Q-TOF-MS

1 | INTRODUCTION

In the early 1970s and 1980s, medical abortion became an alternative way for early termination of pregnancy (Regina et al., 2011). Mifepristone combined with misoprostol is the preferred clinical approach for the induction of abortion (Klaira & Paul, 2020), but the severe side effects of incomplete medical abortion still reached 15% (Ma et al., 2016). Abnormal uterine bleeding (AUB) is a common characteristic in incomplete medical abortion, with an incidence of approximately 3%–30% among reproductive-aged women (Munro et al., 2018). The use of estrogen, tranexamic acid, multi-dose compound contraceptive, and multi-dose progesterone regimen are common clinically available non-surgical options for AUB (Bradley & Gueye, 2015), but these treatments may cause multiple side effects (Yujie et al., 2018).

Angelica sinensis (Oliv.) Diels (Danggui) was widely used as a functional food or a dietary supplement in Asia, Europe, and America. It is also a famous traditional Chinese medicine for the treatment of anemia, dysmenorrhea, premenstrual, menopausal syndrome, and other gynecological diseases (Ma et al., 2015). Previous research indicates that polysaccharides, volatile oils, and organic acids are the main bioactive ingredients of *A. sinensis*. (Jin et al., 2016; Wei et al. 2016). The results of pharmacological studies indicated that *A. sinensis* can replenish and invigorate blood, prevent pain, and moisten the intestines (Ma et al., 2016). In addition, *A. sinensis* also have anti-arrhythmic effects, enhanced immune function, cardioprotective effects, anti-atherosclerotic effects, and inhibiting platelet aggregation (Gu et al., 2016). However, few reports focus on the underlying therapeutic effects and mechanisms of *A. sinensis* for AUB.

Metabolomics is a technique to study the metabolites and their dynamic changes before and after being stimulated or disturbed for the biological system (e.g., after a specific gene variation or environmental change). Metabolomics has been widely used in plant molecular phenotype (Showkat et al., 2019), drug safety (Chen et al., 2021; Yu et al., 2018), molecular pathology (Yang & Lao, 2019), mechanism of drug action (Su et al., 2020), and disease diagnosis (Karakioulaki & Stolz, 2019). In addition, it was also used to evaluate the impact of storage environment on food quality (Guo et al., 2019). Metabolomics is considered to be a useful strategy to explain the underlying mechanisms of TCM for the treatment of diseases. It emphasizes the study objects (humans or animals) as a unified whole, which is in accordance with the principle of integrity and dynamics of Traditional Chinese Medicine (TCM). The analysis methods of metabolomics mainly include nuclear magnetic resonance spectroscopy (NMR), gas chromatography-mass spectrometry (GC-MS), and liquid chromatography-mass spectrometry (LC-MS). Among all of the analytical technologies, UPLC-Q-TOF-MS is becoming a key technology in biomarker discovery (Gika et al., 2014).

In the present study, the concentration of main active substances in AWE was determined and the chemical components were identified by UPLC-Q-Exactive Orbitrap-MS/MS. The coagulation function, serum hormone levels, H&E staining, and immunohistochemistry observation of uterus were detected after the intervention of AWE. An UPLC-Q-TOF-MS method and multivariate analysis were applied to identify the potentially authentic biomarkers. The purpose of this study was to reveal the underlying mechanisms of AWE for the treatment of AUB and to provide a theoretical basis for clinical application.

2 | MATERIALS AND METHODS

2.1 | Chemicals and reagents

Angelica sinensis was harvested in Longxi County, Gansu Province in July 2019, and identified by Prof. Ying Liu (School of preclinical medicine, Chengdu University). Ferulic acid (batch No. MUST-20060511) was brought from Chengdu Mansite Biotechnology Co., Ltd. Senkyunolide A (batch No. wkq20050703) was brought from Sichuan Weikeqi Co., Ltd. Ligustilide (batch No. G01001909022) was brought from Chengdu Ruifensi Biotechnology Co., Ltd. Mifepristone and Misoprostol were brought from Zizhu Pharmaceutical Co. (Peking, China). Pg ELISA kit (batch No. VE3AZJHQ1W) and E_2 ELISA kit (batch No. 44IBV1FHE5) were brought from Elabscience Biotechnology Co., Ltd (Wuhan, China). HCG ELISA kit (batch No. 11/2019) was brought from Shanghai MLBIO Biotechnology Co., Ltd. (Shanghai, China). Antibody against ERα (batch No. 00,046,360), Antibody against ERβ (batch No. 00,053,760), and Antibody against PR (batch No. 00,235,360) were brought from Abcam Co., Ltd. (Shanghai, China). HRP (batch No. 20,200,528) was brought from Bioss Co., Ltd. (Peking, China). PBS (batch No. 20,190,307) was brought from Zsbio Co., Ltd. (Peking, China). DAB (batch No. 07,062,019) was brought from Baso Co., Ltd. (Zhuhai, China).

2.2 | Preparation of the water extract of *Angelica sinensis*

The water extract of *A. sinensis* (AWE) was extracted by heating reflux method. Thirty grams of crude herbal drugs was added to purified water ten times and extracted for twice (v/w), each extraction time was 30 min. The concentration of AWE was 0.6 g/ml after filtration (expressed by the weight per mL of crude drugs).

2.3 | UPLC-MS analysis of AWE

The analysis was performed in a Thermo Fisher Vanquish UPLC system with a Thermo Fisher Q Exactive (Iowa, USA). The mobile phase consisted of 0.1% formic acid in water (A) and acetonitrile (B). The elution program was as follows: 0–35 min, 95%–5% A; 35–35.01 min, 5%–95% A; and 35.01–40 min, 5% A. C18 column (4.6 × 100 mm, 2.7 μm) was maintained with the temperature of 30°C; flow rate, 0.4 ml/min; injection volume, 1 μl.

The MS operating parameters were as follows: the ion mode was positive; ion spray voltages, 3.5 kV; turbo spray temperature,

320℃; and m/z range, 100–1000. The main chemical constituents of *A. sinensis* were identified according to the exact molecular mass, the cleavage fragments of MS2, the mz cloud, mzVault 2.0 MS database, and literature review.

2.4 | Determination of ferulic acid, senkyunolide A, and ligustilide in AWE by UPLC-MS

The AWE was mixed with 50% methanol (1:1) and filtered through a 0.22 μm membrane filter. The concentration of AWE was 0.022 g/ml after filtration (expressed by the weight per mL of crude drugs).

The analysis was performed using an Vanquish UPLC system with a TSQ Fortis triple quadrupole mass spectrometer (Thermo Fisher, USA), Accucore™ C18 column (2.1mm × 100mm, 2.6 μm, Thermo Fisher, USA). The mobile phase consisted of 0.1% formic acid in water (A) and acetonitrile (B). The UPLC elution program was as follows: 0–5 min, 85%-60% A; 5–10 min, 60%-55% A; 10–18 min, 55%-30% A; 18–18.01 min, 30%-85% A; and 18.01–23 min, 85% A, and Injection volume, 10 μl; flow rate, 0.2 ml/min; column temperature, 35 ℃. The Mass operating parameters were as follows: The ion mode was positive; scan type, SRM; sheath gas flow rate, 35 arb; aux gas flow rate, 15 arb; aux gas heater temp, 350℃; spray voltage, 3.5 kV; and capillary temp, 350℃.

2.5 | Animal experiments

Female Sprague–Dawley (*SD*) rats of specific pathogen-free (SPF) status, weighing 200–220 g; and male *SD* rats of SPF status, weighing 250–300 g (Certificate No. SCXK (Chuan) 2020-030) were brought from the Chengdu Dossy Experimental Animals CO.LTD. (Chengdu, China). The all animals were kept under the same conditions. All experimental protocols were approved by the Animal Ethics Committee of the Chengdu University (20191209-lxsz003).

The AUB rat model was established by mifepristone and misoprostol according to the method of previous literature (Zuo et al., 2019). The pregnancy control group (P) and AUB model group (M) were given with sterile saline, and the AUB + AWE group was administrated with dosage of 2.16 g/kg AWE once a day for 7 days.

2.6 | Histopathological examination

The uterine tissues were immediately dissected after the experiment, removed fat and connective tissue, and fixed in 4% paraformaldehyde solution. Then, the uterine tissues were dehydrated at 4℃ for 24–48 hr, conventionally paraffin embedded, sectioned at 4 μm, and stained with hematoxylin–eosin (HE). Pathological changes of the endometrium were observed and photographed under a microscope.

2.7 | Measurement of serum hormone levels

The serum levels of progesterone (Pg), estradiol (E$_2$), and human chorionic gonadotrophin (HCG) were measured according to the instructions of manufacturer of the ELISA kits, respectively.

2.8 | Detection of plasma coagulation function

Collected blood (3 ml) from the abdominal aorta with sodium citrate at a mass concentration of 3.8 g/L (anticoagulant: blood = 1:9) was centrifuged to obtain plasma. Prothrombin time (PT), thrombin time (TT), activated partial thrombin activity time (APTT), and fibrinogen (FIB) were determined by a hemagglutination analyzer.

2.9 | Protein distribution analyses by immunohistochemistry

The uterine tissues were dehydrated, defatted, and conventionally paraffin embedded. Then, the uterine tissues were sectioned at 4 μm, deparaffinized, and rehydrated. After that, the tissue sections were incubated with 3% H$_2$O$_2$, repaired in antigen recovery solution, and then sealed at room temperature for 20 min after drip-adding normal goat serum blocking solution. Then, the samples were incubated at 4 ℃ overnight with primary inhibitors (dilution 1:200): estrogen receptor α (ERα), estrogen receptor β (ERβ), and progesterone receptor (PR). One day after incubation, the cells were washed with PBS three times for 5 min each time, and then, drip-added and incubated the secondary antibody at room temperature for 1 hr. SABC was added and incubated at 37℃ for 1 hr. Stained the proteins to dark-brown by immersion in diaminobenzidine. The slices were rinsed with deionized water for 10 min. Hematoxylin was used for counterstaining, and hydrochloric acid alcohol was differentiated. Routine dehydration, transparentizing, sealing, and microscopy were performed.

2.10 | Serum sample preparation

Added 400 μl anhydrous acetonitrile containing internal standard into 100 μl serum sample and vortex mixed for 3 min. Then, centrifuged the mixture at 12,000 rpm for 10 min to obtain the supernatant and putted it into a sampling vial.

2.11 | UPLC-Q-TOF-MS analysis conditions

An UPLC-Q-TOF-MS system (Agilent, USA) was used for analysis with a BEH C18 column (2.1 mm × 100 mm, 1.7 μm). 0.1% formic acid in water (A) and acetonitrile (B) was used as a mobile phase with the following elution program: 0–3 min, 10%–30% B, 3–25 min, and 30%–95% B. Column temperature, 35℃; flow rate, 0.35 ml/min. The full scan range was 50 to 1,200 m/z; sheath gas temperature, 320℃;

sheath gas flow, 12 L/min; drying gas temperature, 300℃; drying gas flow, 6 L/min; capillary voltage, 3.5 kV; and nebulizer pressure, 1.0 bar.

2.12 | Data processing

The partial least-squares discriminant analysis (PLS-DA) and orthogonal partial least-squares discriminant analysis (OPLS-DA) were used for data analysis. The database used to identify the potential biomarkers was as follows: https://hmdb.ca/, http://www.lipidmaps.org/, http://www.genome.jp/kegg/, http://metlin.scripps.edu/. All results were described as the mean $\pm$ standard deviation (*SD*). One-way analysis of variance (ANOVA) was used to analyze study data for significance comparison.

3 | RESULTS

3.1 | Identification of major compounds in AWE

The representative chromatography was shown in Figure 1. Twenty-six constituents were identified by the accurate mass and relative ion abundance of the target peaks. The main constituents in AWE were γ-Aminobutyric acid (GABA), Nystose, L-Valine, Nicotinic acid, 4-Oxoproline, Guanosine, Succinic acid, L-Phenylalanine, DL-Tryptophan, 2-Anisic acid, Isophthalic acid, Caffeic acid, L-Histidine, N-Acetyl-D-alloisoleucine, Vanillin, Isofraxidin, Ferulic acid, Azelaic acid, Coniferyl aldehyde, Berberine, Jatrorrhizine, Coptisine chloride, Palmatine, Ligustilide, Senkyunolide A, and Levistilide A. The area percentage of the constituents is shown in Table 1.

3.2 | Determination of ferulic acid, senkyunolide A, and ligustilide in AWE

The representative chromatography was shown in Figure 2. Ferulic acid was linear over a concentration range of 3.10–154.90 μg/ml, senkyunolide A was linear at 1.33–40.00 μg/ml, and ligustilide was linear at 2.04–254.65 μg/ml. The concentration of the mixed reference solution was taken as the abscisic coordinate, and the peak area was taken as the ordinate for linear regression. Typical equation of calibration curve for ferulic acid was $y = 14333x + 63,294$ ($r = 0.9970$); the curve of senkyunolide A was $y = 343389x - 340450$ ($r = 0.9978$); and that of ligustilide was $y = 88,686x + 876,354$ ($r = 0.9953$). The contents of ferulic acid, senkyunolide A, and ligustilide were 0.7276, 0.0868, and 1.9908 mg/g, respectively.

3.3 | AWE improved the histopathological damage

Microscopic examination explored that the endometrium of the P group was significantly thickened, the uterine cavity was small, the glands and blood vessels in the lamina propria were rich and dilated, and some of them were hyperemic (Figure 3a). Compared with the P group, the endometrium was thin, with local defects, and the lamina propria was mainly showed densely distributed blood vessels with slight congestion in the M group (Figure 3b). The endometrium in the AWE group was rich in blood vessels and loose in the stroma, but the symptoms were less severe than those in the model group (Figure 3c).

3.4 | Measurement of serum hormone levels

Comparing with the P group, the E_2, Pg, and HCG levels were significantly decreased in the M group ($p < .01$). The E_2 and Pg levels were significantly increased with the treatment of AWE ($p < .05$) (Figure 4a–c).

3.5 | Effects of AWE on blood coagulation function in rats

Compared with the P group, the APTT and TT levels were significantly longer and FIB level was significantly lower in the M group ($p < .05$). The APTT and TT levels were significantly lower, and FIB level was significantly longer with the treatment of AWE ($p < .05$). (Figure 5).
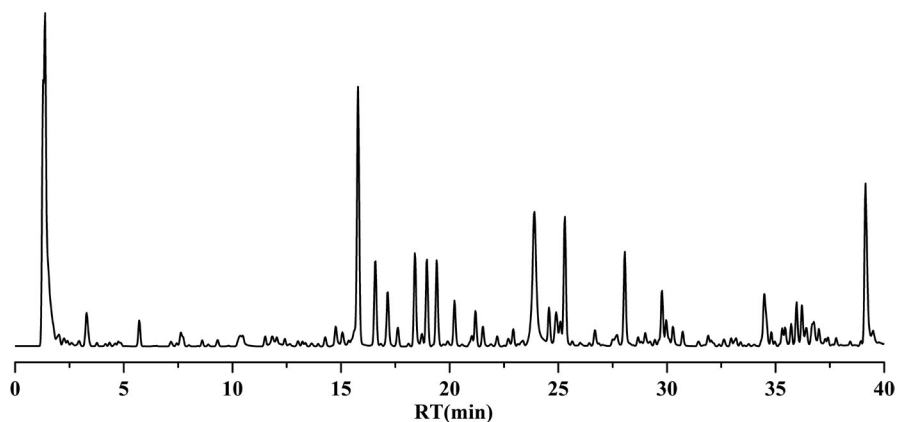

FIGURE 1 The total ion chromatograms of samples by UPLC-MS

TABLE 1 The information of compounds identified in AWE by UPLC-MS

Peak	Constituent	Formula	Molecular Weight	RT (min)	Area(Max.)	M/Z	Fragments
1	γ-Aminobutyric acid (GABA)	$C_4H_9NO_2$	103.0639	2.500	1.12E+09	104.0714	87.04505
2	Nystose	$C_{24}H_{42}O_{21}$	666.2216	2.563	1.51E+08	711.2197	665.21375,485.15158,341.10703,221.06606,179.05527,89.02335
3	L-Valine	$C_5H_{11}NO_2$	117.0795	2.734	4.18E+08	118.0867	72.08173,55.05518
4	Nicotinic acid	$C_6H_5NO_2$	123.0328	3.298	2.58E+08	124.0395	96.05189,80.05059
5	4-Oxoproline	$C_5H_7NO_3$	129.0417	3.427	3.28E+08	128.0345	82.02883
6	Guanosine	$C_{10}H_{13}N_5O_5$	283.0923	4.155	1.59E+09	284.0998	152.05748
7	Succinic acid	$C_4H_6O_4$	118.0258	4.250	8.39E+07	117.0185	73.02842
8	L-Phenylalanine	$C_9H_{11}NO_2$	148.0530	5.404	1.48E+09	166.0869	120.08154,103.05509
9	DL-Tryptophan	$C_{11}H_{12}N_2O_2$	204.0919	6.996	3.04E+09	188.0725	146.06157,118.06660
10	2-Anisic acid	$C_8H_8O_3$	152.0467	7.592	2.45E+08	151.0394	123.04420,107.04922,93.03354
11	Isophthalic acid	$C_8H_6O_4$	166.0260	8.380	1.24E+09	165.0186	121.02848
12	Caffeic acid	$C_9H_8O_4$	180.0420	9.202	8.76E+08	179.0347	135.04422,71.01277
13	L-Histidine	$C_6H_9N_3O_2$	155.0688	9.876	7.35E+07	154.0616	137.03474,110.07134,93.04478
14	N-Acetyl-D-alloisoleucine	$C_8H_{15}NO_3$	173.1048	10.273	1.52E+07	172.0974	130.08641
15	Vanillin	$C_8H_8O_3$	152.0467	11.346	9.69E+07	151.0394	136.01569
16	Isofraxidin	$C_{11}H_{10}O_5$	222.0529	11.967	3.23E+07	221.0455	206.02150,190.99799,163.00291,135.00803
17	Ferulic acid	$C_{10}H_{10}O_4$	194.0574	12.226	7.56E+07	193.0503	178.02640,134.03628
18	Azelaic acid	$C_9H_{16}O_4$	188.1044	13.153	3.51E+08	187.0971	125.09621,97.06487
19	Coniferyl aldehyde	$C_{10}H_{10}O_3$	178.0626	13.573	8.28E+07	177.0553	162.03142
20	Berberine	$C_{20}H_{17}NO_4$	335.1177	13.627	4.55E+07	336.1250	320.09439,292.09912
21	Jatrorrhizine	$C_{20}H_{19}NO_4$	337.1354	13.691	9.45E+08	338.1427	322.11090,308.09509,294.11551,280.09985
22	Coptisine chloride	$C_{19}H_{14}ClNO_4$	319.0885	13.998	8.28E+07	320.0958	292.09979
23	Palmatine	$C_{21}H_{21}NO_4$	351.1500	15.186	1.86E+08	352.1573	336.12640,308.13129
24	Ligustilide	$C_{12}H_{14}O_2$	190.0996	22.968	1.80E+08	191.1065	173.09673,145.10168,117.07053,91.05499
25	Senkyunolide A	$C_{12}H_{16}O_2$	192.1150	23.990	2.08E+08	193.1222	175.11226,147.11722,137.06015,105.07059,91.05498
26	Levistilide A	$C_{24}H_{28}O_4$	380.1986	32.075	4.40E+08	381.2062	191.10716

3.6 | Effects of AWE on ERα, Erβ, and PR levels in rats

Expression of ERα, Erβ, and PR was reduced in the M group when compared to the P group ($p < .01$). The expression of ERα and ERβ was increased with the treatment of AWE ($p < .05$). (Figure 6a–c).

3.7 | Data quality assurance of UPLC-Q-TOF-MS

The typical total ion current chromatograms of each group of serum samples were shown in Figure 7.

3.8 | Differential metabolites between the AUB and the pregnancy rats

The PLS-DA and OPLS-DA analyses explored that there was an obvious separation between the P, M, and AWE groups (Figure 8a,b). The S-plots indicated the contribution of different metabolites variables between the P and M groups (Figure 8c). Fourteen significantly differential metabolites were shown in Table 2. LysoPC (20:5), Glycine, N-Acetyl-leukotriene E4, PC (18:1(9Z)/18:1(9Z)), LysoPC (18:3), LysoPC (18:0/0:0), Leukotriene D5, 20-Oxo-leukotriene E4, LysoPC (17:0), Sphinganine, LysoPC (18:2), LysoPC (16:0), L-Valine, and N-Lactoylleucine were significantly lower in the M group compared

FIGURE 2 The chromatogram of mixed reference solution and AWE by UPLC-MS. (a) Mixed reference solution, (b) AWE. 1. Ferulic acid, 2. Senkyunolide A, 3. Ligustilide
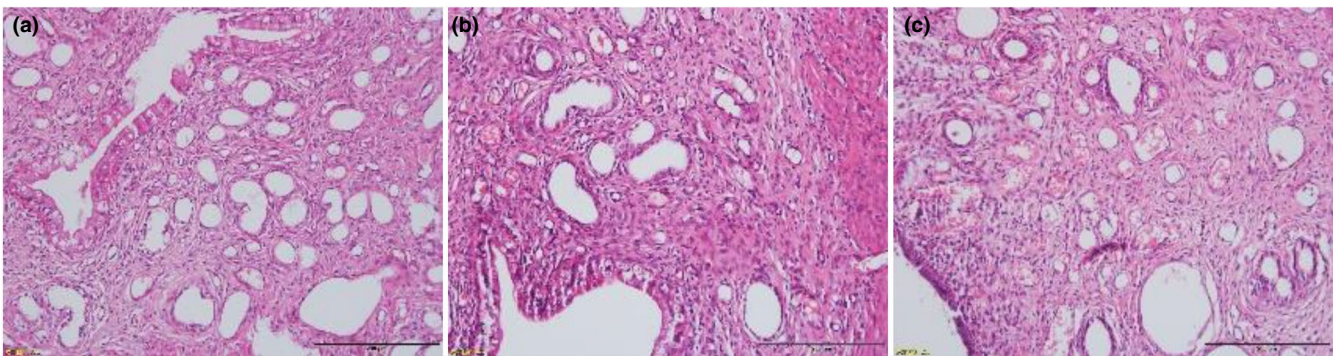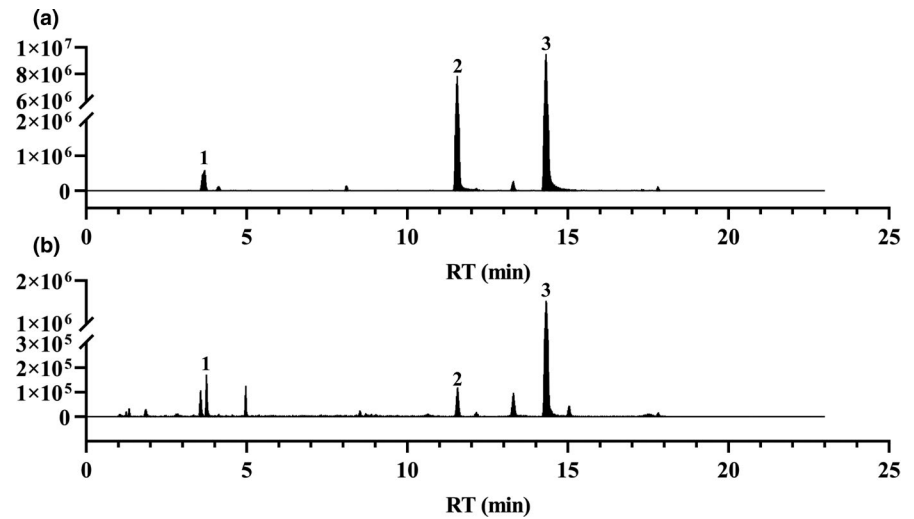

FIGURE 3 Effects of AWE on pathological changes of endometrium in rats by HE Staining (200×). (a) Pregnant group, (b) AUB model group, (c) AWE group
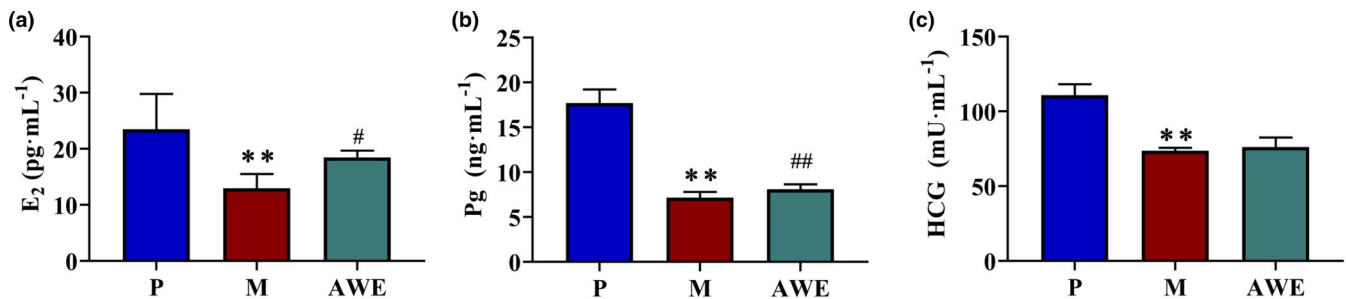

FIGURE 4 The E$_2$, Pg, and HCG Levels in each group. (a) E$_2$, (b) Pg, (c) HCG. The results were presented as the mean ± SD, $n = 6$. **$p < .01$ AUB model group versus pregnant group, #$p < .05$ AWE group versus AUB model group, ##$p < .01$ AWE group versus medical aborting group

with the P group (Figure 9). The metabolism pathways of glycine, serine and threonine, glyoxylate and dicarboxylate, glycerophospholipid, primary bile acid biosynthesis, glutathione, and sphingolipid were significantly altered in the M group (Figure 10).

3.9 | Differential metabolites between AUB and AWE treatment rats

There was a significant separation between the M and AWE groups in the OPLS-DA model (Figure 11a), indicating that AWE had an effect on the metabolic profile of AUB rats. The S-plots indicated the contribution of different metabolites variables between the M and AWE groups (Figure 11b). Twenty-one significantly differential metabolites were shown in Table 3, and there showed that the specific changes of the relative content in these specific metabolites (Figure 12). LysoPC (20:5), Glycine, N-Acetyl-leukotriene E4, PC (18:1(9Z)/18:1(9Z)), LysoPC (18:3), LysoPC (18:0/0:00), Leukotriene D5, 3-Hydroxybutyric acid, 20-Oxo-leukotriene E4, Hippuric acid, LysoPC (17:0), D-Leucine, and L-Valine were significantly higher in the AWE group compared with the M group. However, the other metabolites, including D-Glucuronic acid, All-trans-Retinoic acid, and
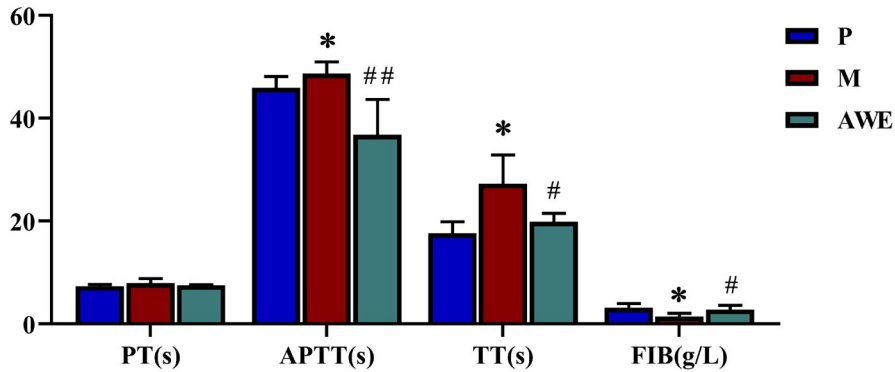
FIGURE 5 The four coagulation indices of each experimental group. The results were presented as the mean ± SD, $n = 6$. *$p < .05$ AUB model group versus pregnant group, #$p < .05$ AWE group versus AUB model group, ##$p < .01$ AWE group versus AUB model group
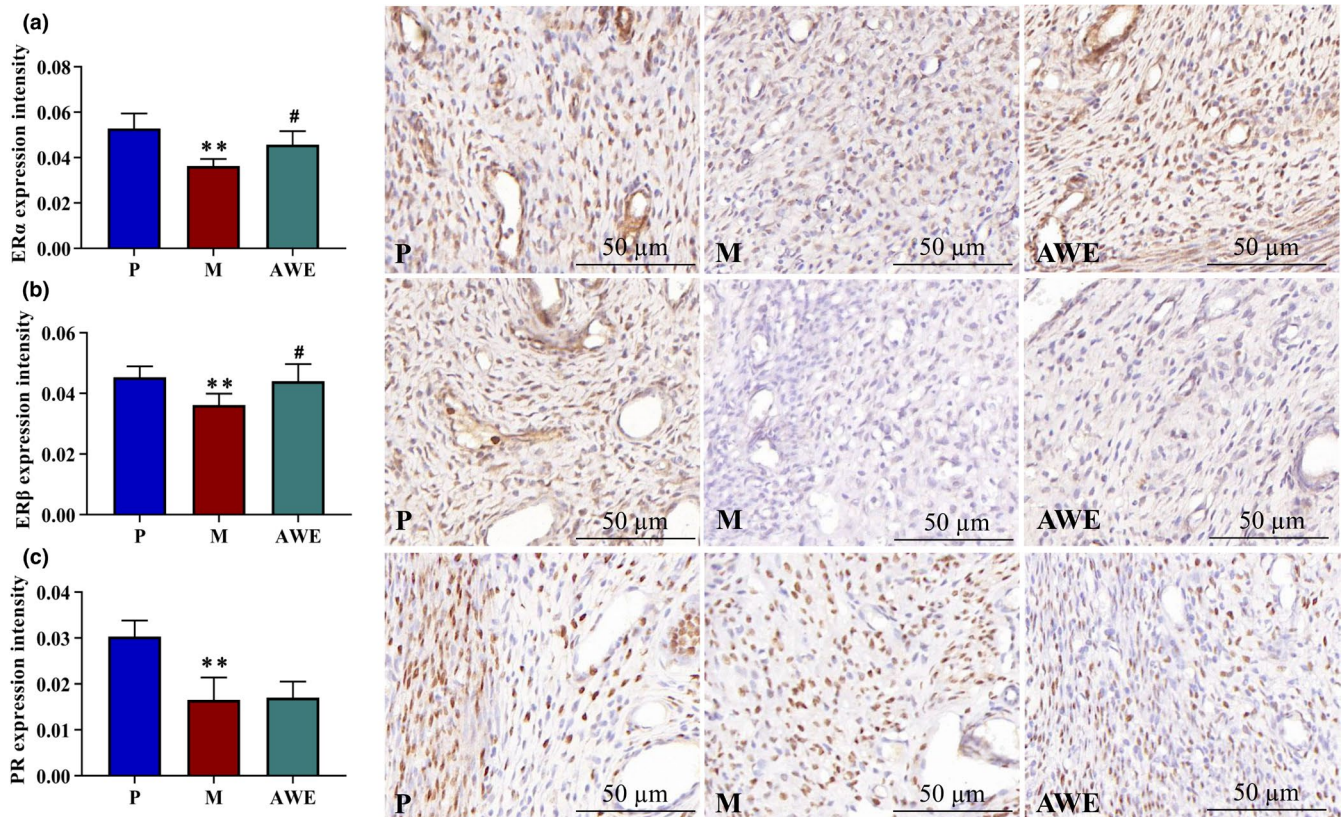

FIGURE 6 The ERα, Erβ, and PR Levels in each group. (a) ERα, (b) ERβ, (c) PR. The results were presented as the mean ± SD, $n = 6$. **$p < .01$ AUB model group versus pregnant group, #$p < .05$ AWE group versus AUB model group
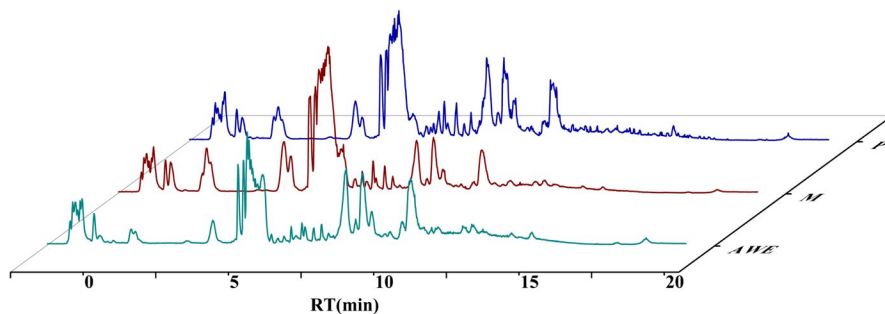

FIGURE 7 The typical total ion chromatography of all serum samples in positive mode. P: Pregnant group, M: AUB model group, AWE: AWE group

25-Hydroxyvitamin D3, were significantly lower in the AWE group compared with the M group. The metabolism pathways of primary bile acid biosynthesis, pentose and glucuronate interconversions, glycerophospholipid, glutathione, glyoxylate and dicarboxylate, sphingolipid, glycine, serine and threonine, retinol, ascorbate, and aldarate were significantly altered in the M group (Figure 13).
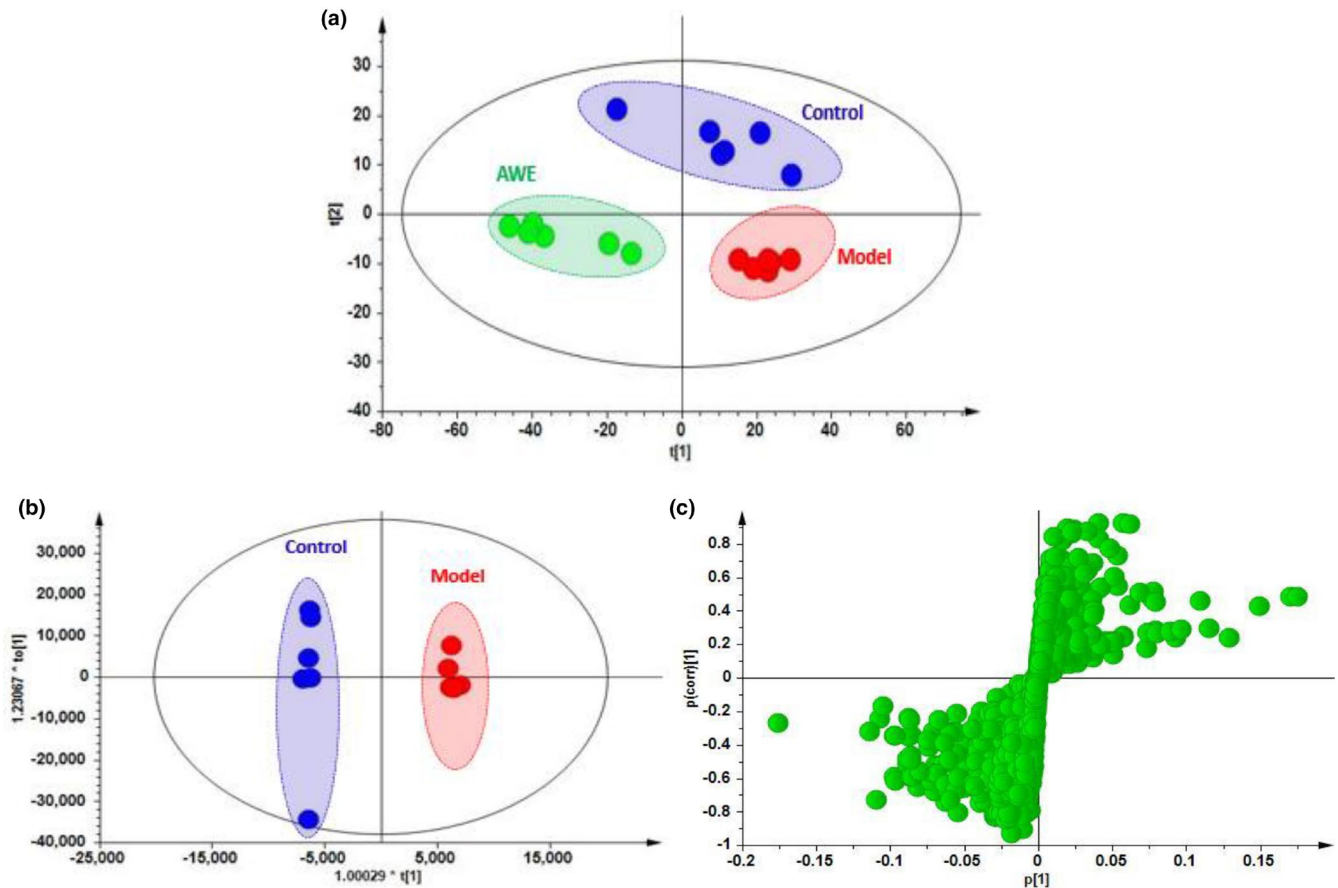
FIGURE 8 The multivariate statistical analysis. (a) PLS-DA; (b) OPLS-DA; (c) OPLS-DA s-plot

TABLE 2 14 Differential metabolites in the serum of P and M groups

Compound	Formula	Metabolites	M/Z	Rt (min)	VIP
A1	$C_{28}H_{48}NO_7P$	LysoPC (20:5)	542.3176	9.604	4.6232
A2	$C_{26}H_{43}NO_9S$	Glycine	546.3472	10.749	3.5524
A3	$C_{25}H_{39}NO_6S$	N-Acetyl-leukotriene E4	482.3185	11.836	1.7062
A4	$C_{44}H_{84}NO_8P$	PC (18:1(9Z)/18:1(9Z))	786.5852	16.334	2.3486
A5	$C_{26}H_{48}NO_7P$	LysoPC (18:3)	518.3189	9.676	3.8540
A6	$C_{26}H_{54}NO_7P$	LysoPC (18:0/0:0)	524.3638	12.447	1.2658
A7	$C_{25}H_{38}N_2O_6S$	Leukotriene D5	495.3220	9.898	2.3342
A8	$C_{23}H_{35}NO_6S$	20-Oxo-leukotriene E4	454.2870	10.300	1.2371
A9	$C_{25}H_{52}NO_7P$	LysoPC (17:0)	510.3476	11.330	1.8070
A10	$C_{18}H_{39}NO_2$	Sphinganine	302.2703	8.897	1.3561
A11	$C_{26}H_{50}NO_7P$	LysoPC (18:2)	520.3303	11.049	3.1960
A12	$C_{24}H_{50}NO_7P$	LysoPC (16:0)	496.3338	10.884	10.9197
A13	$C_5H_{11}NO_2$	L-Valine	118.0849	0.937	2.9892
A14	$C_9H_{17}NO_4$	N-Lactoylleucine	204.1198	1.003	5.7701

4 | DISCUSSION

Angelica sinensis, as a medicinal food, has widely been used for the treatment of amenorrhea, dysmenorrheal, and premenstrual syndrome of gynecological disorders (Li et al., 2012). Studies have shown A. *sinensis* contains ferulic acid, senkyunolide A, ligustilide, etc., so it was speculated that AWE had a certain influence on the anti-inflammatory (Fang et al., 2020), blood replenishing (Tao
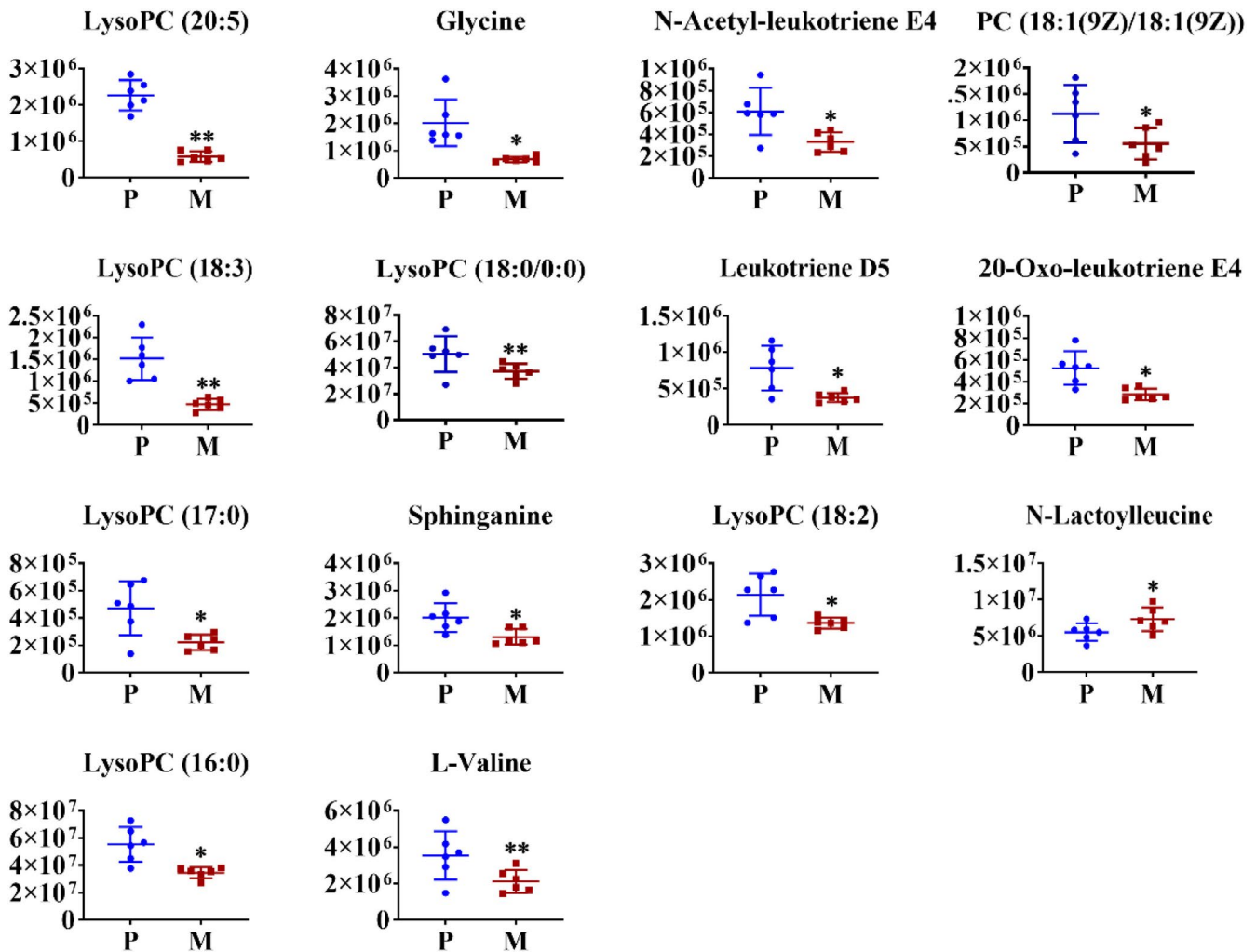
FIGURE 9 The relative intensities of the examined metabolites obtained from P and M groups. The results were presented as the mean ± SD, $n = 6$. $*p < .05$ versus pregnant group, $** p < .01$ versus pregnant group
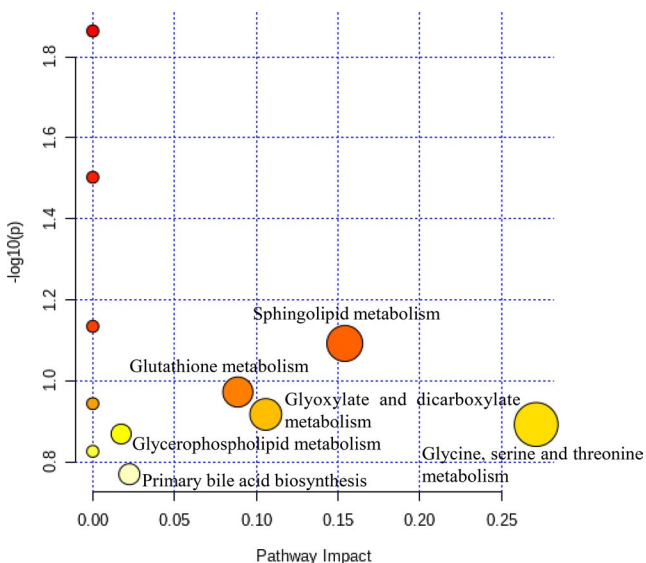

FIGURE 10 Summary of pathway analysis of P and M groups

et al., 2016), liver lipid accumulation, and fatty regeneration (Ma et al., 2020). Peng Cao et al. found *Angelica sinensis* polysaccharide as a kind of "tonic foods," which has potential to be used as a hepatoprotective agent for Acetaminophen-induced hepatic damage (Cao et al., 2018). Yong li Hua et al. found that *A. sinensis* can promote hematopoiesis, enhance antiapoptotic effects, and regulate energy metabolism (Hua et al., 2017). Qin Fan et al. found that ferulic acid could scavenge PPH- and ABTS-free radicals, while ligustilide exhibited scavenging capacity for ABTS-free radicals (Fan et al., 2020). Zi-wen Yuan et al. found that *A. sinensis* intervention could significantly relieve blood stasis syndrome in rats (Yuan et al., 2019). In this study, APTT and TT levels were significantly lower in AWE group ($p < .05$), the APTT and TT levels were significantly lower, and FIB level was significantly longer with the treatment of AWE, indicating that *A. sinensis* can regulate blood coagulation function of AUB rats.

Metabolomics is a large-scale research technology that uses modern analytical method to assess the creature physiological status in different conditions (Wei et al., 2020). The metabolic profiles reflect an individual's function state at a certain point, which
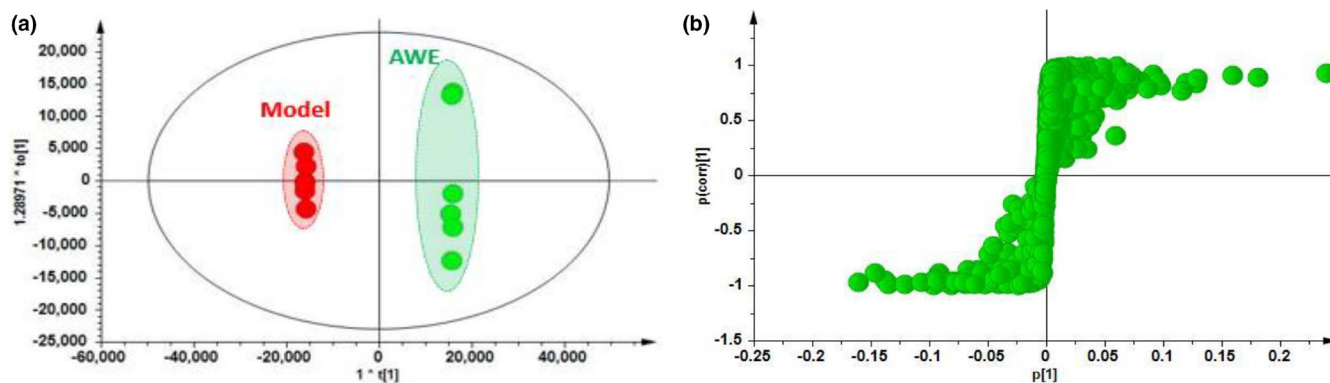
FIGURE 11 The results of multivariate statistical analysis from the serum samples. LC-MS positive (a and b), (a) OPLS-DA; (b) OPLS-DA s-plot

TABLE 3 21 Differential metabolites in the serum of M and AWE groups

Compound	Formula	Metabolites	M/Z	Rt (min)	VIP
B1	$C_{28}H_{48}NO_7P$	LysoPC (20:5)	542.3176	9.604	1.7704
B2	$C_{26}H_{43}NO_9S$	Glycine	546.3472	10.749	1.6321
B3	$C_{25}H_{39}NO_6S$	N-Acetyl-leukotriene E4	482.3185	11.836	1.3480
B4	$C_{44}H_{84}NO_8P$	PC (18:1(9Z)/18:1(9Z))	785.5852	16.334	1.7397
B5	$C_{26}H_{48}NO_7P$	LysoPC (18:3)	518.3189	9.676	1.1027
B6	$C_{26}H_{54}NO_7P$	LysoPC (18:0/0:0)	524.3638	12.447	11.0291
B7	$C_{25}H_{38}N_2O_6S$	Leukotriene D5	495.3220	9.898	1.1269
B8	$C_4H_8O_3$	3-Hydroxybutyric acid	105.0338	4.681	1.0865
B9	$C_{23}H_{35}NO_6S$	20-Oxo-leukotriene E4	454.2870	10.300	1.2019
B10	$C_9H_9NO_3$	Hippuric acid	180.0650	4.681	1.2399
B11	$C_{25}H_{52}NO_7P$	LysoPC(17:0)	510.3476	11.330	1.3592
B12	$C_{18}H_{39}NO_2$	Sphinganine	302.2703	8.897	1.4056
B13	$C_{26}H_{50}NO_7P$	LysoPC(18:2)	520.3303	11.049	2.0366
B14	$C_9H_{17}NO_4$	N-Lactoylleucine	204.1198	1.003	1.6609
B15	$C_{18}H_{34}O_2$	Oleic acid	283.1748	5.656	2.7529
B16	$C_6H_{10}O_7$	D-Glucuronic acid	195.1221	1.815	4.0168
B17	$C_{20}H_{28}O_2$	all-trans-Retinoic acid	301.2044	5.656	4.2104
B18	$C_{24}H_{50}NO_7P$	LysoPC(16:0)	496.3338	10.884	2.4304
B19	$C_{27}H_{44}O_2$	25-Hydroxyvitamin D3	401.3184	7.223	8.3933
B20	$C_6H_{13}NO_2$	D-Leucine	132.1005	0.927	3.4918
B21	$C_5H_{11}NO_2$	L-Valine	118.0849	0.937	4.1642

is consistent with the integrality and systematicness of traditional Chinese medicine (Bao et al., 2017). This technique has been used to study the effects of Chinese medicine syndrome patterns (Fengxia et al., 2010; Li et al., 2016). As an important part of the human body, blood contains abundant information and is often used as the matrix for metabolomics research. Therefore, the UPLC-Q-TOF-MS metabolomics platform and multivariate statistical analysis method were used to assess the rats' serum to reveal the mechanism of AWE in AUB caused by incomplete abortion. In our study, we identified 21

potential biomarkers that were directly or indirectly correlated for the therapeutic effects of AWE in AUB caused by incomplete abortion, mainly including amino acids, retinol, fatty acids, and lysophospholipids. We have found that the serum of the incomplete medical abortion rats showed altered metabolism mainly in amino acid, retinol, lipid metabolism and primary bile acid biosynthesis pathways.

Amino acids are necessary for embryonic growth and development. In our study, we found that the level of some amino acids including glycine, D-leucine, and L-valine was abnormal in the AWE
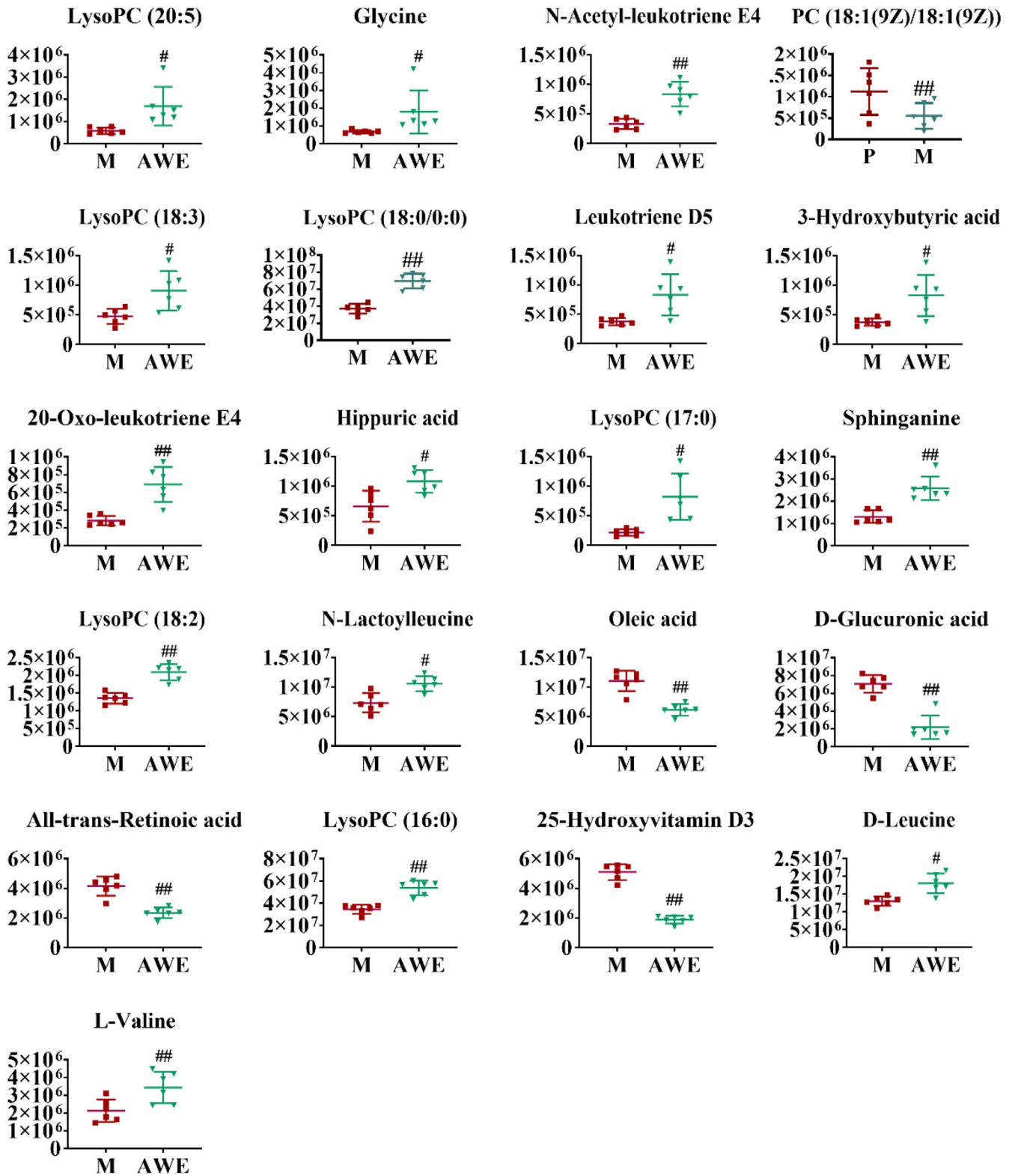
FIGURE 12 The relative intensities of the examined metabolites obtained from M and AWE groups. The results were presented as the mean ± SD, n = 6. #p < .05 versus. AUB model group, ## p < .01 versus AUB model group

group. Glycine was closely associated with inflammation among these amino metabolites (Angélica et al., 2014). Glycine promotes myelin phagocytosis and the production NO and TNF-α, which may affect immunological processes of inflammatory diseases (Carmans

et al., 2010). In the inflammation, the TNF-α induces protein decomposition and catabolism to up-regulate the urea synthesis (Louise et al., 2013). Yong-li Hua et al. found that volatile oil from *A. sinensis* can inhibit inflammation through down-regulating the synthesis
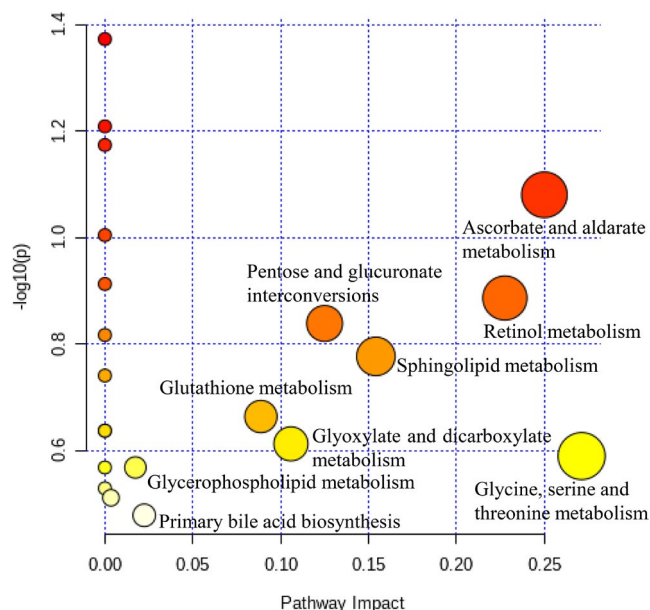
FIGURE 13 Summary of pathway analysis of M and AWE groups

of glycine, arachidonic acid, L-glutamate, pyruvate, and succinate (Angélica et al., 2014). D-Leucine and L-valine are branched chain amino acids (BCAAs), especially leucine, and can enhance protein synthesis through the mTOR signaling pathway to regulate energy balance, which plays a vital role in blastocyst development. Banerjee et al. found that the metabolites, including lysine, L-arginine, glutamine, threonine, histidine, phenylalanine, and tyrosine, were significantly increased in patients with idiopathic recurrent spontaneous miscarriage, which may be involved in vascular dysfunction associated with poor endometrial receptivity and excessive inflammatory reactions (Priyanka et al., 2014). Houghton et al. used reversed-phase high-performance liquid chromatography (RHPLC) and found that the content of leucine was significantly reduced after in vitro fertilization when the embryo developed into the cyst embryo culture medium, while the contents of valine and isoleucine were significantly reduced in the embryo culture medium that did not develop into the blastocyst. Valine and isoleucine have a definite influence on embryo development (Houghton et al., 2002). Zhang et al. found that BCAAs are closely involved in pregnancy outcome. The elevated BCAAs can clearly impair the development of diploids cells to the morula and blastocyst stages (Thuan et al., 2002). Xiao-yao Miao et al. used metabolomic-based gas chromatography-mass spectrometry and pattern recognition to study the potential mechanism of Danggui Buxue Tang's anti-fatigue effect on weight-bearing forced swimming mice and found that Danggui Buxue Tang had a good anti-fatigue effect (Miao et al., 2018). In our study, we found that the glycine, D-leucine, and L-valine serum concentrations in the AWE group were higher than those in the M group, which may indicate that *Angelica sinensis* may affect the inflammatory process in AUB rats.

Lipid metabolism mainly consists of linoleic acid, glycerophospholipid, and sphingolipid metabolism. Oleic acid, which is closely

related to leukotriene synthesis, is considered to be a key factor in tissue injury, inflammation, and vasoconstriction. Kim et al. found that the water extract of *Angelica sinensis* has an anti-inflammatory effect via the NO-burst/calcium-mediated JAK-STAT pathway (Young-Jin et al., 2018). Yao et al. found that the anti-inflammatory activity of the volatile oil of *Angelica sinensis* mainly through regulating glycine and arachidonic acid metabolic disorders (Yao et al., 2015). And in our study, after AWE intervention, the AWE group showed significant upregulation of N-Acetyl-leukotriene E4, 20-Oxo-leukotriene E4, and Leukotriene D5, which indicated that the effect of AWE on rats with AUB may involve the regulation of arachidonic acid metabolic network disorders. Lyso PC, a phospholipid, can regulate vascular tone and induce endothelial dysfunction. It is reported that saturated fatty acids can induce the expression of cyclooxygenase (Akito et al., 2009) and promote the synthesis of PGF2α (Helliwell et al.,). In this study, LysoPC (16:0), LysoPC (17:0), PC (18:1(9Z)/18:1(9Z)), LysoPC (18:2), LysoPC (18:3), LysoPC (20:5), and LysoPC (18:0/0:00) were up-regulated in the AWE group. These results indicate that glycerophospholipid metabolism was abnormal.

Sphinganine is a sphingolipid that is involved in the formation of cell membranes. It can be phosphorylated under the catalysis of sphingosine kinase to produce a potent signaling lipid molecule, sphingosine-1-phosphate (S1P). S1P can regulate the physiological functions of cell survival, growth, proliferation, and apoptosis from the extracellular receptor pathway and the intracellular second messengers. Roth et al. indicated that sphingosine-1-phosphate can promote the maturation of bovine oocytes and enhance the development of embryos (Roth & Hansen, 2004). Hannoun et al. indicated that the fragmentation rate of human preimplantation embryos medium with S1P was significantly lower and the embryos quality was better (Antoine et al., 2010). In our study, we found that the serum concentration of sphingosine in the AWE group was higher than that in the M group, which may be because AWE has a regulatory effect on sphingosine.

All-trans-retinoic acid belongs to vitamin A (retinol), which is a basic nutrient required for mammalian reproduction. This molecule plays a vital role in promoting the normal development of embryos, regulating cell proliferation and differentiation, and maintaining normal cell differentiation and immune system function integrity. Ueda et al. showed that chemical signaling induced by the use of retinoic acid can promote the differentiation of embryonic stem cells into neurons (Ueda et al., 2018). In our study, we found that the level of all-trans-retinoic acid was down-regulated in the AWE group. In summary, AWE could adjust the abnormal metabolism state of amino acid, retinol, and lipid metabolism with AUB induced by incomplete medical abortion.

5 | CONCLUSIONS

An UPLC-Q-TOF-MS-based serum metabolomic approach was applied to investigate the mechanisms of AWE for the treatment of AUB. Twenty-one potential biomarkers were eventually identified,

which may be involved in the intervention mechanism of AWE for the treatment of AUB. Some metabolic pathways including primary bile acid biosynthesis, glycerophospholipid metabolism, pentose and glucuronate interconversions, glutathione metabolism, glyoxylate and dicarboxylate metabolism, sphingolipid metabolism, glycine, serine and threonine metabolism, retinol metabolism, ascorbate, and aldarate metabolism were altered by AWE treatment. The significantly reversed the metabolic aberrations in AUB group by AWE facilitates to support the therapeutic effect and potential mechanisms of AWE on AUB induced by incomplete medical abortion.

CONFLICT OF INTEREST

The authors declare no conflict of interest.

DATA AVAILABILITY STATEMENT

The data that support the findings of this study are available from the corresponding author upon reasonable request.

ORCID

Yan Zhang 🆔 https://orcid.org/0000-0002-5026-7446

REFERENCES

Akito, K., Yo, T., Hiroyasu, H., Hideki, K., & Makoto, K. (2009). Different impacts of saturated and unsaturated free fatty acids on COX-2 expression in C(2)C(12) myotubes. _American Journal of Physiology. Endocrinology and Metabolism_, _297_(6), E1291–E1303. https://doi.org/10.1152/ajpendo.00293.2009

Angélica, R. R., Ely, O. B., Guillermo, C. S., Eulises, D. D., & Mohammed, E. H. (2014). Glycine restores glutathione and protects against oxidative stress in vascular tissue from sucrose-fed rats. _Clinical Science (London)_, _126_(1), 19–29. https://doi.org/10.1042/CS20130164

Antoine, H., Ghina, G., Antoine, A. M., Tony, G. Z., Fatiha, H., & Johnny, A. (2010). Addition of sphingosine-1-phosphate to human oocyte culture medium decreases embryo fragmentation. _Reproductive Biomedicine Online_, _20_(3), 328–334. https://doi.org/10.1016/j.rbmo.2009.11.020

Bao, Y., Wang, S., Yang, X., Li, T., Xia, Y., & Meng, X. (2017). Metabolomic study of the intervention effects of Shuihonghuazi Formula, a Traditional Chinese Medicinal formulae, on hepatocellular carcinoma (HCC) rats using performance HPLC/ESI-TOF-MS. _Journal of Ethnopharmacology_, _198_, 468–478. https://doi.org/10.1016/j.jep.2017.01.029

Bradley, L. D., & Gueye, N. A. (2015). The medical management of abnormal uterine bleeding in reproductive age women. _American Journal of Obstetrics & Gynecology_, S0002937815008455, https://doi.org/10.1016/j.ajog.2015.07.044

Cao, P., Sun, J., Sullivan, M. A., Huang, X., Wang, H., Zhang, Y., Wang, N., & Wang, K. (2018). Corrigendum to "_Angelica sinensis_ polysaccharide protects against acetaminophen-induced acute liver injury and cell death by suppressing oxidative stress and hepatic apoptosis in vivo and in vitro" [Int. J. Biol. Macromol. 111 (May 2018) 1133–1139]. _International Journal of Biological Macromolecules_, _115_, 1269. https://doi.org/10.1016/j.ijbiomac.2018.04.168

Carmans, S., Hendriks, J. J. A., Thewissen, K., Van den Eynden, J., Stinissen, P., Rigo, J.-M., & Hellings, N. (2010). The inhibitory neurotransmitter glycine modulates macrophage activity by activation of neutral amino acid transporters. _Journal of Neuroscience Research_, _88_(11), 2420–2430. https://doi.org/10.1002/jnr.22395

Chen, L., Jiang, E., Guan, Y., Xu, P., Shen, Q., Liu, Z., Zhu, W., Chen, L., Liu, H., & Dong, H. (2021). Safety of high-dose Puerariae Lobatae Radix in adolescent rats based on metabolomics. _Food Sciences and Nutrition_, _9_(2), 794–810. https://doi.org/10.1002/fsn3.2044

Fan, Q., Yang, R., Yang, F., Xia, P., & Zhao, L. (2020). Spectrum-effect relationship between HPLC fingerprints and antioxidant activity of _Angelica sinensis_. _Biomedical Chromatography_, _34_(2), e4707. https://doi.org/10.1002/bmc.4707

Fang, C., Yu, Z., Qiang, L., Fang, Z., & Kaiping, W. (2020). Inhibition of dextran sodium sulfate-induced experimental colitis in mice by _Angelica sinensis_ polysaccharide. _Journal of Medicinal Food_, _23_(6), 584–592. https://doi.org/10.1089/jmf.2019.4607

Gika, H. G., Theodoridis, G. A., Plumb, R. S., & Wilson, I. D. (2014). Current practice of liquid chromatography–mass spectrometry in metabolomics and metabonomics. _Journal of Pharmaceutical and Biomedical Analysis_, _87_, 12–25. https://doi.org/10.1016/j.jpba.2013.06.032

Guo, X., Luo, T., Han, D., & Wu, Z. (2019). Analysis of metabolomics associated with quality differences between room-temperature- and low-temperature-stored litchi pulps. _Food Sciences and Nutrition_, _7_(11), 3560–3569. https://doi.org/10.1002/fsn3.1208

Helliwell, R. J. A., Adams, L. F., & Mitchell, M. D. (2004). Prostaglandin synthases: Recent developments and a novel hypothesis. _Prostaglandins, Leukotrienes, and Essential Fatty Acids_, _70_(2), 101–113. https://doi.org/10.1016/j.plefa.2003.04.002

Houghton, F. D., Hawkhead, J. A., Humpherson, P. G., Hogg, J. E., Balen, A. H., Rutherford, A. J., & Leese, H. J. (2002). Non-invasive amino acid turnover predicts human embryo developmental capacity. _Human Reproduction_, _17_(4), 999–1005. https://doi.org/10.1093/humrep/17.4.999

Hua, Y., Yao, W., Ji, P., & Wei, Y. (2017). Integrated metabonomic–proteomic studies on blood enrichment effects of _Angelica sinensis_ on a blood deficiency mice model. _Pharmaceutical Biology_, _55_(1), 853–863. https://doi.org/10.1080/13880209.2017.1281969

Jin, Y., Qu, C., Tang, Y., Pang, H., Liu, L., Zhu, Z., Shang, E., Huang, S., Sun, D., & Duan, J.-A. (2016). Herb pairs containing Angelicae Sinensis Radix (Danggui): A review of bio-active constituents and compatibility effects. _Journal of Ethnopharmacology_, _181_, 158–171. https://doi.org/10.1016/j.jep.2016.01.033

Karakioulaki, M., & Stolz, D. (2019). Biomarkers in pneumonia-beyond procalcitonin. _International Journal of Molecular Ences_, _20_(8), 2004. https://doi.org/10.3390/ijms20082004

Klaira, L., & Paul, P. D. (2020). Current and potential methods for second trimester abortion. Best practice & research. _Clinical Obstetrics & Gynaecology_, _63_, 24–36. https://doi.org/10.1016/j.bpobgyn.2019.05.006

Li, M., Shu, X., Xu, H., Zhang, C., Yang, L., Zhang, L., & Ji, G. (2016). Integrative analysis of metabolome and gut microbiota in diet-induced hyperlipidemic rats treated with berberine compounds. _Journal of Translational Medicine_, _14_(1), 237. https://doi.org/10.1186/s12967-016-0987-5

Li, W., Guo, J., Tang, Y., Wang, H., Huang, M., Qian, D., & Duan, J.-A. (2012). Pharmacokinetic comparison of ferulic acid in normal and blood deficiency rats after oral administration of _Angelica sinensis_, Ligusticum chuanxiong and their combination. _International Journal of Molecular Sciences_, _13_(3), 3583-3597. https://doi.org/10.3390/ijms13033583

Louise, T. K., Niels, J., Buch, M. A., Kristian, A. N., Henning, G., Juul, H. J., & Hendrik, V. (2013). Regulation of urea synthesis during the acute-phase response in rats. _American Journal of Physiology._

Gastrointestinal and Liver Physiology, *304*(7), G680–686. https://doi.org/10.1152/ajpgi.00416.2012

Ma, C., Feng, W. H., Han, W. T., Lu, Y. P., Liu, W., Sui, Y., Zhao, N., Lye, S. J., & Li, J. X. (2016). Elevated mRNA expression of PGF2 receptor splice variant 2(FP-V2) in human decidua is associated with incomplete mifepristone-misoprostol-induced early medical abortion by regulation of interleukin-8. *Journal of Maternal-Fetal & Neonatal Medicine*, *29*(21), 3472–3477. https://doi.org/10.3109/14767058.2015.1132692

Ma, J. P., Guo, Z. B., Jin, L., & Li, Y. D. (2015). Phytochemical progress made in investigations of *Angelica sinensis* (Oliv.) Diels. *Chinese Journal of Natural Medicines*, *13*(4), 241–249. https://doi.org/10.1016/S1875-5364(15)30010-8

Ma, P., Sun, C., Li, W., Deng, W., Adu-Frimpong, M., Yu, J., & Xu, X. (2020). Extraction and structural analysis of *Angelica sinensis* polysaccharide with low molecular weight and its lipid-lowering effect on non-alcoholic fatty liver disease. *Food Science & Nutrition*, *8*(7), 3212–3224. https://doi.org/10.1002/fsn3.1581

Miao, X., Xiao, B., Shui, S., Yang, J., Huang, R., & Dong, J. (2018). Metabolomics analysis of serum reveals the effect of Danggui Buxue Tang on fatigued mice induced by exhausting physical exercise. *Journal of Pharmaceutical and Biomedical Analysis*, *151*, 301–309. https://doi.org/10.1016/j.jpba.2018.01.028

Munro, M. G., Critchley, H. O. D., & Fraser, I. S. (2018). The two FIGO systems for normal and abnormal uterine bleeding symptoms and classification of causes of abnormal uterine bleeding in the reproductive years: 2018 revisions. *International Journal of Gynecology & Obstetrics*, *143*(3), 393–408. https://doi.org/10.1002/ijgo.12666

Priyanka, B., Mainak, D., Sudha, S., Mamata, J., Baidyanath, C., & Koel, C. (2014). (1)H NMR serum metabonomics for understanding metabolic dysregulation in women with idiopathic recurrent spontaneous miscarriage during implantation window. *Journal of Proteome Research*, *13*(6), 3100–3106. https://doi.org/10.1021/pr500379n

Regina, K., Nathalie, K., Metin, G. A., Justus, H. G., Linan, C., & Aldo, C. (2011). Medical methods for first trimester abortion. *The Cochrane Database of Systematic Reviews*, *11*, CD002855. https://doi.org/10.1002/14651858.CD002855.pub4

Roth, Z., & Hansen, P. J. (2004). Sphingosine 1-phosphate protects bovine oocytes from heat shock during maturation. *Biology of Reproduction*, *71*(6), 2072–2078. https://doi.org/10.1095/biolreprod.104.031989

Showkat, A. G., Kutubuddin, A. M., & Robert, H. (2019). Advances in understanding salt tolerance in rice. *Theor Appl Gene*, *132*(4), 851–870. https://doi.org/10.1007/s00122-019-03301-8

Su, M., Cao, G., Wang, X., Daniel, R., Hong, Y., & Han, Y. (2020). Metabolomics study of dried ginger extract on serum and urine in blood stasis rats based on UPLC-Q-TOF/MS. *Food Sciences and Nutrition*, *8*(12), 6401–6414. https://doi.org/10.1002/fsn3.1929

Tao, W., Hong-Guo, S., Yong-Li, H., Peng-Ling, L., & Yan-Ming, W. (2016). Urine metabonomic study for blood-replenishing mechanism of *Angelica sinensis* in a blood-deficient mouse model. *Chinese Journal of Natural Medicines*, *14*(03), 210–219. https://doi.org/10.1016/S1875-5364(16)30018-8

Thuan, N. V., Harayama, H., & Miyake, M. (2002). Characteristics of preimplantational development of porcine parthenogenetic diploids relative to the existence of amino acids in vitro. *Biology of Reproduction*, *67*(6), 1688–1698. https://doi.org/10.1095/biolreprod.102.004812

Ueda, K., Onishi, A., Ito, S.-I., Nakamura, M., & Takahashi, M. (2018). Generation of three-dimensional retinal organoids expressing rhodopsin and S- and M-cone opsins from mouse stem cells. *Biochemical and Biophysical Research Communications*, *495*(4), 2595–2601. https://doi.org/10.1016/j.bbrc.2017.12.092

Wei, Q., Li, J., Zhan, Y., Zhong, Q., Xie, B., Chen, L., Chen, B., & Jiang, Y. (2020). Enhancement of glucose homeostasis through the PI3K/Akt signaling pathway by dietary with Agaricus blazei Murrill in STZ-induced diabetic rats. *Food Science & Nutrition*, *8*(2), 1104–1114. https://doi.org/10.1002/fsn3.1397

Wei, W., Zeng, R., Gu, C., Qu, Y., & Huang, L. (2016). *Angelica sinensis* in China-A review of botanical profile, ethnopharmacology, phytochemistry and chemical analysis. *Journal of Ethnopharmacology*, *190*, 116–141. https://doi.org/10.1016/j.jep.2016.05.023

Yang, M., & Lao, L. (2019). Emerging applications of metabolomics in traditional Chinese medicine treating hypertension: Biomarkers, pathways and more. *Frontiers in Pharmacology*, *10*, 158. https://doi.org/10.3389/fphar.2019.00158

Yao, W., Zhang, L., Hua, Y., Ji, P., Li, P., Li, J., Zhong, L., Zhao, H., & Wei, Y. (2015). The investigation of anti-inflammatory activity of volatile oil of *Angelica sinensis* by plasma metabolomics approach. *International Immunopharmacology*, *29*(2), 269–277. https://doi.org/10.1016/j.intimp.2015.11.006

Young-Jin, K., Young, L. J., Hyun-Ju, K., Do-Hoon, K., Hee, L. T., Suk, K. M., & Wansu, P. (2018). Anti-inflammatory effects of *Angelica sinensis* (Oliv.) diels water extract on RAW 264.7 induced with lipopolysaccharide. *Nutrients*, *10*(5), 647. https://doi.org/10.3390/nu10050647

Yu, J., He-jian, L., & Cheng-qiang, F. (2018). Transcriptome-metabolomics analysis and its application in studying drug action mechanism. *Biotechnology Bulletin*, *34*(12), 68–76.

Yuan, Z., Zhong, L., Hua, Y., Ji, P., Yao, W., Ma, Q., Zhang, X., Wen, Y., Yang, L., & Wei, Y. (2019). Metabolomics study on promoting blood circulation and ameliorating blood stasis: Investigating the mechanism of *Angelica sinensis* and its processed products. *Biomedical Chromatography*, *33*(4), e4457. https://doi.org/10.1002/bmc.4457

Yujie, S., Su, L., Yun, C., & Xiumei, S. (2018). Chinese herbal medicines for the treatment of non-structural abnormal uterine bleeding in perimenopause: A systematic review and a meta-analysis. *Complementary Therapies in Medicine*, *41*, 252–260. https://doi.org/10.1016/j.ctim.2018.09.021

Zuo, C., Zhang, Y., Wang, J., Han, L., Peng, C., & Peng, D. (2019). Deciphering the intervention mechanism of Taohong Siwu Decoction following the abnormal uterine bleeding rats based on serum metabolic profiles. *Journal of Pharmaceutical and Biomedical Analysis*, *170*, 204–214. https://doi.org/10.1016/j.jpba.2019.03.051